



Effects of Added Mass on Indirect Structural Health Monitoring of Bridges

Richard May¹ , Thomas Reynolds¹ , Hwa Kian Chai¹ , Robert Corbally² , Abdollah Malekjafarian² , and Yong Lu¹ 

¹ The University of Edinburgh, Edinburgh, Scotland
rich.may@ed.ac.uk

² University College Dublin, Dublin, Ireland

Abstract. The concept of using vehicles as dynamic exciters and sensor carriers for indirect Structural Health Monitoring (iSHM) of bridges has gained considerable interest in recent years. Proposed frameworks typically rely on the assumption that there will be a time and cost benefit in comparison to the temporary or permanent installation of sensors fixed directly to the subject bridge structure. However, the indirect approach suffers from drawbacks including artefacts related to environmental and operational variation (EOV), the mitigation of which is a major ongoing research effort worldwide. The presence of other vehicles during the traversal of the sensor-carrying vehicle contributes to EOV but has received little attention to date. Acting as sprung masses, these additional vehicles can change the effective and observable modal parameters of the bridge. Mitigating this with temporary road closures is contrary to the low-cost high-value minimal-interruption goal of iSHM.

This paper presents initial outcomes from a programme of laboratory-scale physical testing and Finite Element (FE) modelling, aiming to increase knowledge of the effects of additional vehicles on the visibility of bridge modal parameters and damage.

Keywords: Bridge · Indirect monitoring · Traffic · EOV

1 Introduction

This project presents analysis of laboratory-scale tests in which an instrumented test vehicle traversed a bridge under a variety of added mass configuration conditions. By leveraging data simultaneously gathered from bridge- and vehicle-mounted sensors, a comparison of the target and indirectly estimated modal parameters can be achieved.

Yang and Lin's 2004 study [1] modelled vehicles as sprung masses and showed analytically that their dynamic response when traversing bridges (modelled as simply-supported beams) contained information relating to bridge modal frequencies. Later studies have explored various ways to leverage the moving vehicle acceleration response to better illuminate changes in bridge properties related to

damage. The method has been demonstrated in laboratory models and recently at full scale in the field utilising smartphone sensors [2]. Nevertheless, it is recognised that the confounding effects of EOV remain a challenge for iSHM [3]. Included in these effects is the presence of traffic on the subject bridge during traversal of the instrumented sensor-carrying vehicle. The background traffic can be conceptualised as a procession of sprung masses, whose parameters, speed and spacing may vary. Kim et al. [4] report a study where the presence of vehicle mass was confounding to extraction of bridge modal frequency estimates. It is recognised that multi-lane spatial-temporal traffic flow is complex and nonlinear [5]. Equally spaced loads can induce resonance or cancellation phenomena [6] but individual vehicles may or may not traverse a bridge with equal speed and spacing. Adding sprung masses is known to affect the dynamic characteristics of a structure, dependent on mass and frequency ratios, as in the case of tuned mass dampers. Background traffic has been suggested as helpful in iSHM [7] by increasing bridge acceleration amplitude and thus offering a more favourable signal-to-noise ratio for the moving sensor. On the other hand, many studies implicitly require that sensor-carrying vehicles can traverse the bridge in the absence of background traffic. This latter assumption is at odds with the general goal of iSHM: to gather information of high value at low acquisition cost, without excessive disruption. If a bridge must be (even partially) closed to traffic for monitoring purposes, it may be more fruitful to temporarily fix sensors directly to the bridge structure, thereby avoiding many of the potential pitfalls of iSHM. The authors therefore believe there is a need to improve the viability of iSHM methods by better understanding the effects of other vehicles, moving or static, present on a bridge during monitoring.

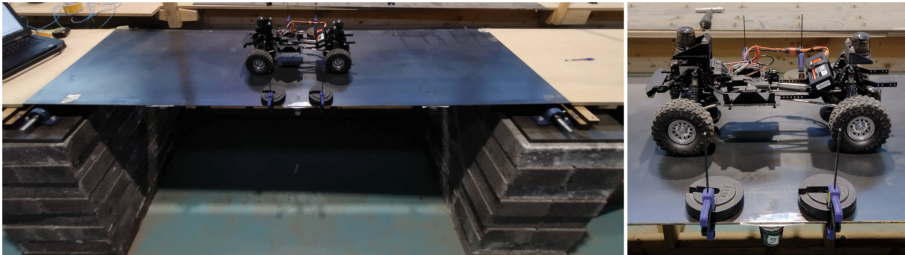


Fig. 1. The physical laboratory model of vehicle and bridge at University College Dublin. Left: general view showing bridge span and model vehicle. Right: detail of vehicle showing accelerometers installed and additional masses clamped to deck.

2 Methodology

This paper is based on physical testing of a scale bridge model and radio-controlled scale vehicle model, and associated FE modelling. The model bridge

and vehicle are the same used by Corbally and Malekjafarian who provide further description [8]. In summary, the bridge comprised a steel plate on pinned supports, stiffened on the underside by steel angles connected by bolts to the plate. The vehicle is a 1/10th scale *SCX10 iii* model by Axial Adventure. Data were collected from wireless triaxial accelerometers: *G-Link-200 8G* by Lord Microstrain. Eight sensors were magnetically fixed to the underside of the bridge deck in an array with sensors at approximately mid, quarter, three-quarter, one-sixth and five-sixths span positions. Four sensors were fixed to 3D-printed stiffened brackets attached to the vehicle at positions suited to record displacement of the front and rear axles and cabin. Data were collected from multiple traversals of the vehicle across the bridge. Additional static masses were clamped to the bridge deck in some testing regimes to simulate the mass of other static vehicles on the bridge. An overview of the laboratory testing arrangement is illustrated in Fig. 1.

The work presented here comprised system identification for so-called *unloaded* (no added static mass) bridge, static vehicle, and combined static vehicle-bridge systems with or without added static mass; FE modelling to further explore the possible effects of parameter variation for the combined static system including the presence of bridge deck damage; inspection of the frequency content from bridge and vehicle-mounted sensors during moving vehicle traversals; and synthetic moving vehicle traversal data used to explore the influence of parameter variation in the presence of bridge deck localised damage.

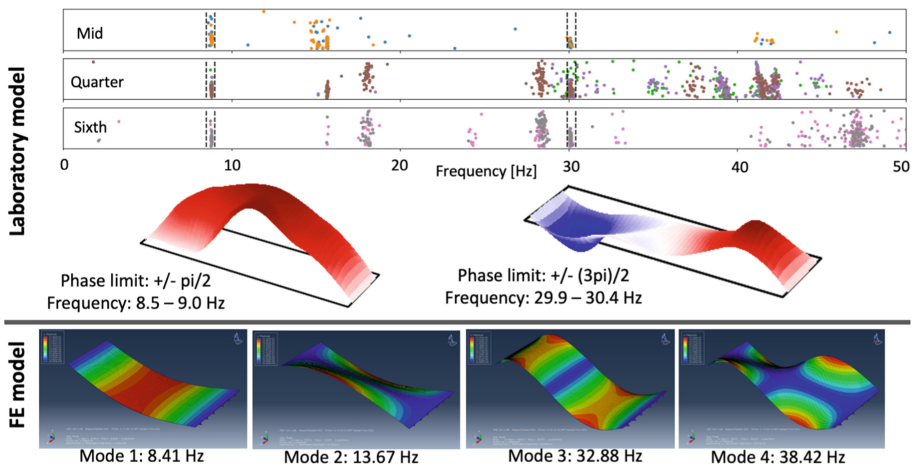


Fig. 2. Identified modal parameters of the laboratory and Finite Element bridge models. Top: clusters of frequency estimates identified using the Matrix Pencil method applied to data gathered from physical model response to impulse excitation. Middle: 2- and 3-dimensional mode shapes estimated from this data for the first two bending modes. Bottom: first four modes identified from Finite Element model.

3 Observations and Discussion

3.1 Bridge and Vehicle Individual System Identification

Mode shapes and associated frequencies were first estimated for the unloaded bridge structure. Impulse loads were applied (hammer taps) at a variety of locations and the acceleration response was used to generate estimates of modal parameters using the Matrix Pencil method, a time-domain curve fitting paradigm outlined by Hua and Sarkar [9]. Figure 2 shows the outcomes of this, including mode shapes for the first two bending modes, plotted using cubic interpolation. Frequency estimates used for plotting mode shapes were manually selected and are identified in the figure. The first four mode shapes from a fitted three-dimensional FE model are also shown. The FE modelling used *Abaqus* software by Dassault Systèmes Simulia. The model used automatically-generated mesh of C3D8R elements of approximately 0.01 m global size, comprised of an undamped steel material, with frequencies extracted by linear perturbation frequency analysis.

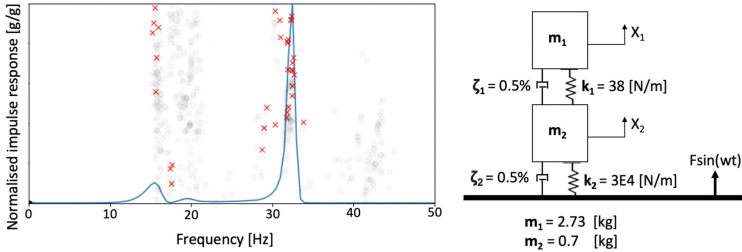


Fig. 3. Vehicle properties estimated from impulse response. Left: front axle accelerometer power spectrum overlaid with frequency estimates generated using Matrix Pencil method. Right: estimated vehicle properties and corresponding 2 DoF model.

Vehicle dynamic system identification was performed in a similar manner, with the vehicle supported on a rigid surface and subject to a variety of hammer taps. Figure 3 shows the power spectrum for the front axle sensor response, overlaid with Matrix Pencil modal frequency estimates. This was manually fitted to a reduced two degree-of-freedom (2 DoF) equivalent model whose parameters and configuration are also shown in the figure. The overall system mass was based on a measured weight for the vehicle. Suspension spring rates were based on the manufacturer’s specifications. The effective tyre stiffness, the distribution of mass between degrees of freedom, and the (assumed orthogonally separable) modal damping were assumed based on visually fitting the observed front axle impulse response to an analytical expression for the response of the idealised system to harmonic base excitation.

3.2 Combined Vehicle-Bridge System Identification

The vehicle-to-bridge mass ratio is in the region of 5%, while the 2 DoF model vehicle’s axle hop frequency is close to the second bending mode frequency of the

bridge. This raises the intriguing possibility of the vehicle interacting with the bridge in a manner similar to a tuned mass damper. To better understand the possible range of effects of vehicle presence, parameters and position, as well as the effects of the presence and location of additional static mass, a programme of system identification was undertaken for the possible combined static vehicle-bridge-mass systems. In this exercise, bridge parameters were estimated based on acceleration impulse response for a variety of static vehicle positions with and without added static mass on the bridge deck.

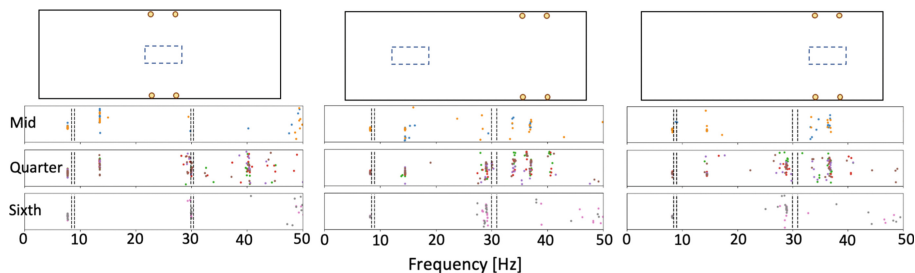


Fig. 4. Illustrative outcomes from system identification for combinations of added mass and static vehicle: Left: vehicle and 4 kg added mass at midspan. Middle: vehicle at quarter span; 4 kg added mass at three-quarter span. Right: vehicle and 4 kg added mass at three-quarter span. Bottom row shows Matrix Pencil modal frequency estimates compared to estimates for unloaded bridge (grey dashed lines).

Three configurations of added static mass were explored: *configuration i* in which no static mass was present; *configuration ii* in which 4 kg was added symmetrically at midspan; and *configuration iii* with 4 kg symmetrically at three quarter-span. An illustrative example of the physical testing is shown in Fig. 4. The first bending mode frequency drops due to the presence of the vehicle and the added mass at midspan, as would be expected. A *mode splitting* effect appears to occur when the vehicle and mass are at quarter- or three quarter-span positions (maximum displacement positions for the expected second bending mode shape).

An equivalent two-dimensional FE model was used to rapidly explore the variation in first and second bending mode frequencies in accordance with varying static vehicle position and added static mass position. The model used an automatically-generated mesh of elements of approximately 0.01 m length, comprised of an undamped steel material, with modal frequencies estimated by linear perturbation frequency analysis. The beam depth and material mass density were chosen to match bending mode frequencies to the three-dimensional FE and physical laboratory models. The vehicle was represented by lumped masses joined by linear spring connectors. Figure 5 shows the outcome of this study, which appears to confirm the first bending mode frequency drop and second bending mode split that were observed in the experimental data. The figure also shows a grey shaded zone; the upper bound representing the expected modal

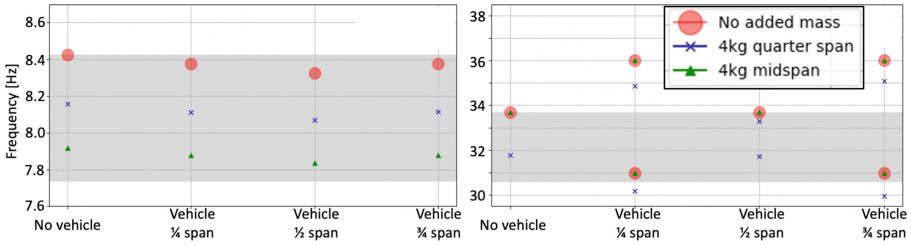


Fig. 5. Finite Element estimates of mode 1 (left) and mode 2 (right) bending frequencies for combined bridge-vehicle system, comparing effects of presence and location of added static mass and position of static vehicle. Grey shaded area indicates expected frequency drop due to damage (modelled as a crack to 50% of section depth located at 30% of span from left support).

frequency for the unloaded bridge in a healthy condition and the lower representing the expected frequency drop due to the presence of bridge damage. This was derived from the FE model. Damage was represented as a reduction in bending stiffness at 30% of the span length from the left support, applied over a short distance and equivalent to a crack extending to 50% of the modelled bridge depth. Inspection of this figure suggests that modal frequencies may vary significantly due to the presence of static vehicles and/or static masses, and that this variation could potentially obscure the frequency changes caused by the substantial level of damage modelled.

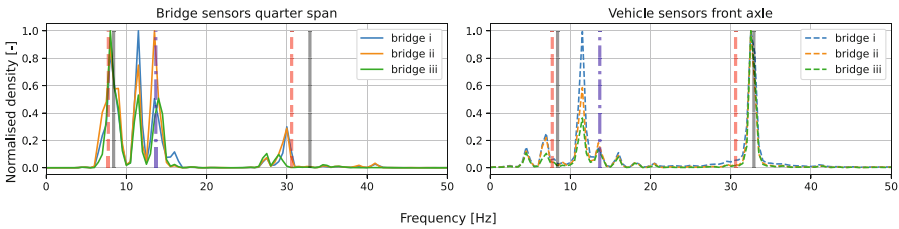


Fig. 6. Comparison of vehicle front axle and bridge quarter span sensor power spectral densities (ensemble averaged for all traversals). Vertical lines indicate FE-derived unloaded bridge frequencies for healthy (solid line) and damaged (dashed line) conditions. Vertical dash-dot line indicates estimated first torsional mode frequency.

3.3 Physical Traversals

For each bridge configuration (i, ii and iii), the acceleration responses of vehicle and bridge were recorded for 20 vehicle traversals at a fixed speed. As an example, Fig. 6 shows the ensemble average power spectral density for the vehicle front axle and bridge quarter-span sensors for all traversals. Expected FE-derived healthy

and damaged bending frequencies are identified by vertical solid grey and dashed red lines, respectively, for the unloaded bridge. The expected (FE-derived) first torsional mode frequency is denoted by a blue vertical dash-dot line. Interestingly this figure does not appear to clearly show any mode splitting behaviour for the second bending mode. Rather, it seems to show a possible mode splitting effect close to the first bending frequency. Additionally, the bridge first torsional mode frequency seems to be clearly present in both vehicle and bridge sensor data. Finally, a strong peak around 32 Hz in the vehicle axle response is observed and is close to the expected vehicle wheel hop and FE-derived bridge bending mode 2 frequencies, but is higher than the mode 2 bending frequency identified from the physical model, raising the possibility of confounding and false positives for frequency identification in this region.

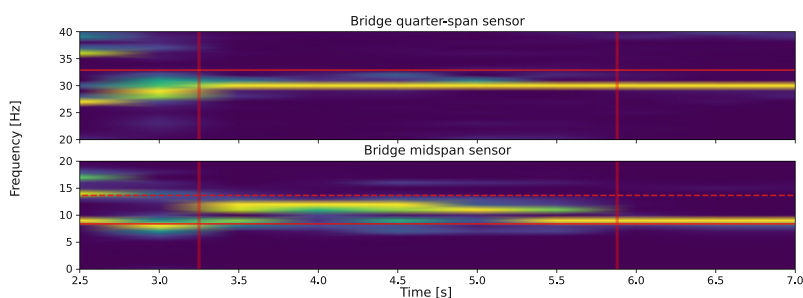


Fig. 7. Example spectrograms for single traversal (unloaded bridge). Top: Bridge quarter span; bottom: bridge midspan. Vehicle-on-bridge time between vertical red lines. Expected unloaded bridge frequencies (FE-derived) shown by horizontal red lines (dashed linetype is torsional frequency).

An example spectrogram for a single traversal (bridge configuration i) is shown in Fig. 7. The plots are normalised to the maximum energy at each timestep in their displayed frequency bands. The vehicle entry and exit from the bridge span is denoted by vertical red lines. Horizontal red lines show the expected FE-derived unloaded bridge first and second bending mode frequencies; a dashed horizontal red line shows the expected first torsional frequency. It is interesting to note that the quarter-span sensor shows the presence of a frequency close to the experimentally-derived second bending mode frequency, but no obviously-apparent mode splitting. The bridge midspan sensor shows what may represent mode splitting behaviour, suggesting the possibility of the vehicle resonating with the bridge in this frequency range (around 7–13 Hz).

Further insight into the time-varying nature of the vehicle-bridge interaction is offered by the plots in Fig. 8. The vehicle-on-bridge time is identified by a red box; inspection of the time-domain acceleration records before this suggests that the bridge behaviour during the traversal may in fact be as a driven dynamic system. The instantaneously-normalised spectrogram in this figure shows that the frequencies present in the vehicle front axle sensor response during the traversal

were already actively contributing to the overall vehicle dynamic behaviour as it progressed towards the bridge span. This further highlights the potential for closely-spaced bridge and vehicle frequencies confounding iSHM.

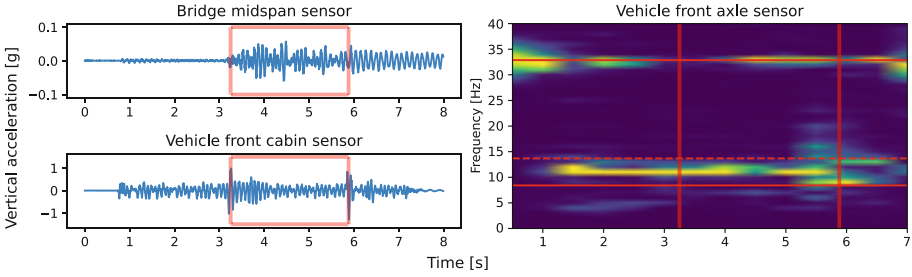


Fig. 8. Left: time domain acceleration response for sample traversal (unloaded bridge). Upper: vehicle front wheel; lower: bridge midspan. Traversal time identified by red outline box. Right: instantaneously normalised vehicle front axle spectrogram. Traversal time delineated by vertical red lines. Expected unloaded bridge frequencies shown by horizontal red lines (dashed linetype is torsional frequency).

3.4 Synthetic Traversals

Outcomes of a parameter variation study are shown in Fig. 9. Acceleration responses for bridge deck and vehicle were synthesised using the two-dimensional FE model. The implicit dynamic analysis was conducted with a fixed-length timestep of 0.004 s. Tangential contact was modelled as frictionless and for normal contact a *hard* pressure-overclosure relationship was adopted. As the previous studies suggested the possibility of tuned mass-type interactions between the bridge second bending mode and the vehicle axle hop frequency, the effect of varying the effective vehicle tyre stiffness was explored.

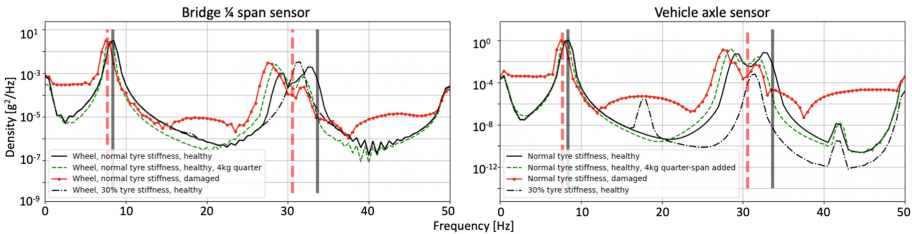


Fig. 9. Power spectral density from Finite Element simulation of vehicle traversal. Virtual sensors on bridge at quarter-span position (left) and vehicle front axle (right). Vertical lines indicate unloaded bridge frequencies for healthy (solid line) and damaged (dashed line) conditions.

A comparison is possible between traversals of a healthy and a damaged bridge. The previously-discussed mode splitting phenomenon appears to be present for the original vehicle configuration and for a vehicle model with a 20% reduction in tyre stiffness. This makes it difficult to clearly observe the second bending mode frequency change associated with damage. Although the models do not show this phenomenon for the first bending mode, the frequency drop caused by damage is difficult to observe clearly as the reduction in tyre stiffness also causes a frequency drop, visible in both vehicle front axle and bridge quarter-span sensor responses. This suggests that the bridge response in this frequency range may be dominated by a driven harmonic from the vehicle. The most clear signal of damage can be seen in the side band regions adjacent to the expected modal frequency peaks, however the modelled large (70%) reduction in tyre stiffness introduces a peak in the power spectrum from the vehicle front axle sensor in the region of 18 Hz, with sufficient signal power to potentially confound efforts to observe the presence of bridge damage using iSHM methods in this particular part of the frequency spectrum.

4 Conclusions and Future Work

The presented preliminary work suggests possible conclusions:

- Within some vehicle-to-bridge mass ratios, the presence of vehicles on a bridge during traversal could potentially change bridge modal frequencies to an extent that obscures changes due to severe damage.
- If bridge and vehicle frequencies are not well-separated, interaction between the sprung mass and the bridge might create spurious frequencies in the bridge response. This could obscure changes caused by severe damage.
- Closely-spaced vehicle and bridge frequencies create the possibility for confounding and false positives in frequency identification even without significant interaction between vehicle and bridge.
- Frequencies present in bridge and vehicle responses during traversals may be strongly driven or dominated by vehicle or bridge excitation prior to the traversal.
- Bridge torsion may interact with vehicle roll modes even when the vehicle is nominally driving along the bridge centreline.
- Information relating to bridge health condition may be visible in the vehicle response spectrum in frequency ranges away from expected modal frequency peaks, but this may be confounded by changes in vehicle properties. False positives are possible, especially in the case of closely-spaced bridge and vehicle frequencies.

Further study is planned or underway to better understand the implications of concurrently-present vehicles for iSHM, including:

- Exploring alternative vehicle models and considering pitch and roll modes.

- Laboratory testing of vehicle traversals in alternative conditions: varying vehicle suspension, further added static mass configurations (including torsional asymmetry) and with prior bridge deck impulse excitation.
- Improving damage detection from vehicle-mounted sensor data by leveraging knowledge of the presence of added masses and static vehicles during traversals in Machine Learning prediction or classification methods.
- Reframing challenges as advantages: exploring the use of tuned vehicle properties to enhance visibility of higher-order bridge modes through resonance.

It should be noted that realisation of vehicle-based indirect bridge monitoring in the field may bring additional challenges which are not present in laboratory-scale models. It would be valuable to repeat and validate the work presented in this paper on a full-scale road bridge.

5 Authorship Contribution and Acknowledgements

Conceptualisation, physical testing, Finite Element simulation, analysis and writing was by Richard May. Project supervision, proofreading and critique was provided by Dr. Hwa Kian Chai, Prof. Yong Lu, and Dr. Thomas Reynolds. Mentoring regarding modal testing and analysis was by Dr. Thomas Reynolds. Python code for implementing the matrix pencil method, and for plotting mode shapes using the estimated modal parameters was adapted from examples provided by colleague Zachariah Wynne, derived from their PhD thesis [10].

Physical testing was conducted in the *Structural Dynamics & Assessment Laboratory* at University College Dublin. Access was kindly facilitated by Abdollah Malekjafarian and assistance and support with testing was provided by Robert Corbally, alongside further proofreading.

This work was supported by the Engineering and Physical Sciences Research Council (grant number: EP/R513209/1).

References

1. Yang, Y.B., Lin, C.W., Yau, J.D.: Extracting bridge frequencies from the dynamic response of a passing vehicle. *J. Sound Vib.* **272**(3–5), 471–493 (2004)
2. Matarazzo, T.J., et al.: Crowdsourcing bridge dynamic monitoring with smart-phone vehicle trips. *Commun. Eng.* **1**(1), 29 (2022)
3. Malekjafarian, A., Corbally, R., Gong, W.: A review of mobile sensing of bridges using moving vehicles: progress to date, challenges and future trends. *Structures* **44**, 1466–1489 (2022)
4. Kim, C.Y., et al.: Effect of vehicle weight on natural frequencies of bridges measured from traffic-induced vibration. *Earthq. Eng. Vib.* **2**, 109–115 (2003)
5. Kerner, B.S.: *The Physics of Traffic*. Springer, Heidelberg (2004). <https://doi.org/10.1007/978-3-540-40986-1>
6. Mao, L., Lu, Y.: Critical speed and resonance criteria of railway bridge response to moving trains. *J. Bridg. Eng.* **18**(2), 131–141 (2013)

7. Lin, C.W., Yang, Y.B.: Use of a passing vehicle to scan the fundamental bridge frequencies: an experimental verification. *Eng. Struct.* **27**(13), 1865–1878 (2005)
8. Corbally, R., Malekjafarian, A.: Bridge damage detection using operating deflection shape ratios obtained from a passing vehicle. *J. Sound Vib.* **537**, 117225 (2022)
9. Hua, Y., Sarkar, T.K.: Matrix pencil method for estimating parameters of exponentially damped/undamped sinusoids in noise. *IEEE Trans. Acoust. Speech Signal Process.* **38**(5), 814–824 (1990)
10. Wynne, Z.: Closing the loop: the integration of long-term monitoring in Engineering design practice. Ph.D. thesis, The University of Edinburgh (2022)